

A numerical study on the seismic behavior of a composite shear wall

Reza Naseri* and Kiachehr Behfarnia^a

Department of Civil Engineering, Isfahan University of Technology, Isfahan 84156-83111, Iran

(Received May 7, 2018, Revised August 19, 2018, Accepted August 20, 2018)

Abstract. Shear walls are one of the important structural elements for bearing loads imposed on buildings due to winds and earthquakes. Composite shear walls with high lateral resistance, and high energy dissipation capacity are considered as a lateral load system in such buildings. In this paper, a composite shear wall consisting of steel faceplates, infill concrete and tie bars which tied steel faceplates together, and concrete filled steel tubular (CFST) as boundary columns, was modeled numerically. Test results were compared with the existing experimental results in order to validate the proposed numerical model. Then, the effects of some parameters on the behavior of the composite shear wall were studied; so, the diameter and spacing of tie bars, thickness and compressive strength of infill concrete, thickness of steel faceplates, and the effect of strengthening the bottom region of the wall were considered. The seismic behavior of the modeled composite shear wall was evaluated in terms of stiffness, ductility, lateral strength, and energy dissipation capacity. The results of the study showed that the diameter of tie bars had a trivial effect on the performance of the composite shear wall, but increasing the tie bars spacing decreased ductility. Studying the effect of infill concrete thickness, concrete compressive strength, and thickness of steel faceplates also showed that the main role of infill concrete was to prevent buckling of steel faceplates. Also, by strengthening the bottom region of the wall, as long as the strengthened part did not provide a support performance for the upper part, the behavior of the composite shear wall was improved; otherwise, ductility of the wall could be reduced severely.

Keywords: composite shear wall; ABAQUS; nonlinear finite element analysis; numerical simulation

1. Introduction

Shear walls, as one of the main structural elements, are used to resist lateral loads imposed on buildings. This structural element is commonly used in two types: 1. Reinforced concrete shear walls, and 2. Steel shear walls.

Using reinforced concrete shear walls in the high-rise buildings, especially in the base floors, leads to thickening shear walls and increasing the density of reinforcement in the boundary elements (Zhang *et al.* 2016). This, in turn, hinders the construction process, leading to heavier structures and a decrease in the usable space of the floors. Additionally, large repeating cycles can result in developing tension cracks in the tension areas and concrete local crushing in the compression zone (Zhang *et al.* 2016). Steel shear walls are another type of lateral load resisting system used in buildings to resist the lateral forces. However, the main defect of these shear walls is steel faceplate buckling in areas exposed to compressive stress, resulting in decreasing stiffness, shear strength, and energy dissipation capacity (Zhang *et al.* 2016).

A practical solution for resisting lateral forces in high-rise buildings is the use of concrete and steel together, which is commonly known as the composite shear wall.

According to Hu *et al.* (2014), Composite shear walls

with concrete and steel plates can be classified into two categories (Fig. 1):

1. Steel plate reinforced concrete (SPRC) composite shear walls
2. Concrete-filled steel plate (CFSP) composite shear walls

CFSP composite shear walls have many advantages. For instance, steel faceplates are used as concrete casting to facilitate the construction process. Additionally, they cover concrete cracks, and also increase concrete and rebar service-life (Hu *et al.* 2014). Also, steel faceplates in two sides of the wall can provide suitable confinement for concrete, resulting in increasing the strength and ductility of the composite shear wall. Such composite walls can be used in nuclear and army installations due to their high resistance against explosive and impact loads. The present study addresses CFSP composite shear walls with CFST boundary elements consisting of steel faceplates, infill concrete and tie bars to create a connection between steel faceplates. As they have many benefits, several numerical and experimental studies have been recently conducted on CFSP composite shear walls. The results of the studies have shown that the ratio of tie bars spacing to steel faceplate thickness has a trivial effect on the initial stiffness and shear walls lateral strength, but reducing this ratio improved the deformation capacity of the composite shear wall (Chen *et al.* 2015). Also, studies conducted by Ji *et al.* (2013) have shown that the thickness of steel faceplates does not influence the composite shear wall ductility significantly and adding circular steel tubes embedded in the CFST boundary elements results in improving the lateral strength

*Corresponding author, Graduate Student

E-mail: r.naseri@cv.iut.ac.ir

^aAssociate Professor

E-mail: kia@cc.iut.ac.ir

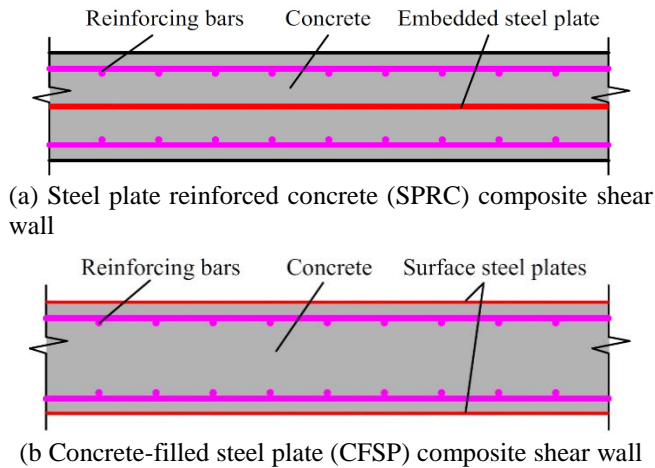
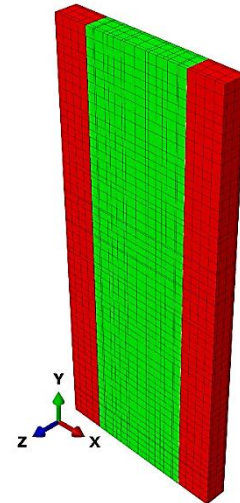


Fig. 1 General details of two steel plate-concrete composite shear walls (Hu *et al.* 2014)

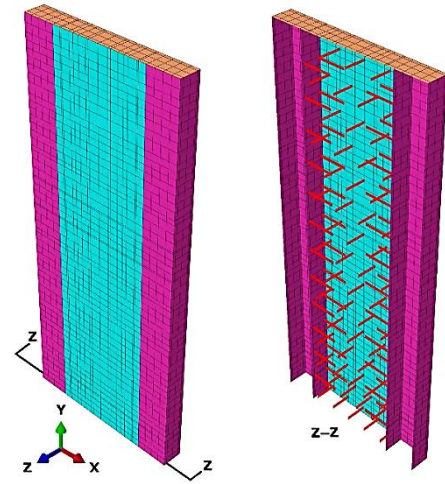
of the shear wall, but does not increase deformation capacity.

Zhang *et al.* (2016) developed an innovative composite shear wall by laying some channels next to each other and casting concrete in the vacant spaces between the segments and tested them under axial and cyclic lateral loading. The results revealed that the presence of steel in the boundary elements had a significant effect on the seismic performance of the composite wall. It means that the increase in the reinforcement of the boundary elements could result in decreasing stiffness and strength degradation and increasing the deformation capacity and energy dissipation capacity of the composite shear wall. Also, tie bars in the boundary elements could prevent local steel buckling and delay fracture and failure; however, they cannot influence the overall wall performance, energy dissipation capacity and deformation capacity. Epackachi *et al.* (2015) simulated the cyclic behavior of four composite shear walls using LS-DYNA and studied the effect of friction between steel faceplates and infill concrete, as well as the effect of the tie bars distribution in the base plate on the overall response of the composite shear walls. The results revealed that the friction coefficient between concrete and steel faceplates did not influence the in-plane cyclic response of the specimens. Rafiei *et al.* (2013) studied the effect of infill concrete compressive strength, the yielding strength of steel faceplates, and the spacing between tie bars on the performance of the composite shear wall using finite element analysis method with ABAQUS software. Huang and Liew (2016) studied the behavior of the composite wall with concrete core, steel faceplates and *J*-hook connectors, under axial compression loads, using the nonlinear finite element analysis. The results showed that the important role of *J*-hook connectors was preventing the local buckling of steel faceplates, due to the lateral expansion of concrete core under compression.

In this paper, a composite shear wall specimen subjected to monotonic lateral load in the presence of axial load was studied numerically using the finite element method; then, the effect of different parameters on its seismic performance was evaluated. This specimen, which had experimentally



(a) Concrete parts (3D elements)



(b) Steel parts (2D elements)

Fig. 2 ABAQUS model of the composite shear wall tested by Ji *et al.* (2013)

been studied by Ji *et al.* (2013), was subjected to cyclic lateral load and compressive axial load.

2. Numerical modeling

Non-linear numerical analysis was applied in order to evaluate the behavior of the composite shear wall using the finite element method by the commercially available software, ABAQUS/Standard (version 6.13). The ABAQUS model of studied composite shear wall is presented in Fig. 2.

2.1 Modeling of concrete

For modeling of concrete, Concrete Damaged Plasticity (CDP) model available in ABAQUS was used. CDP is a comprehensive model based on scalar damage which is capable of simulating the non-linear behavior of concrete subjected to different loading conditions including static, dynamic, cyclic and monotonic ones. In this model, two

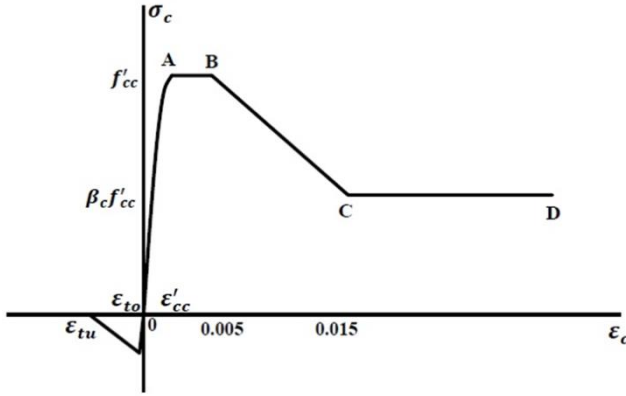


Fig. 3 General stress-strain curve for the confined concrete in CFST beam-columns

mechanisms of fractures for concrete are assumed: cracking tension and compressive crushing (Rafiei 2011, Behfarnia and Shirmeshan 2017). For modeling the non-linear behavior of concrete using CDP, concrete uniaxial stress-strain curves are required in compression and tension. In this paper, to introduce concrete stress-strain curves, a model suggested by Liang (2009) for infill concrete in concrete-filled steel tubular (CFST) beam-columns was used (Fig. 3). In this model, steel tube, by creating confinement for the concrete, increases concrete ductility, but does not enhance its ultimate strength (Liang 2009). In this model, as demonstrated in Fig. 3, the OA part of the stress-strain curve is defined according to Mander *et al.* (1998), as illustrated in Eqs. (1), (2), (3) and (4).

$$\sigma_c = \frac{f'_{cc} \lambda (\epsilon_c / \epsilon'_{cc})}{\lambda - 1 + (\epsilon_c / \epsilon'_{cc})^\lambda} \quad (1)$$

$$\lambda = \frac{E_c}{E_c - (f'_{cc} / \epsilon'_{cc})} \quad (2)$$

$$E_c = 3320 \sqrt{f'_{cc}} + 6900 \text{ (MPa)} \quad (3)$$

$$\epsilon'_{cc} = \begin{cases} 0.002 & f'_{cc} \leq 28 \text{ (MPa)} \\ 0.002 + \frac{f'_{cc} - 28}{54000} & 28 < f'_{cc} \leq 82 \text{ (MPa)} \\ 0.003 & f'_{cc} > 82 \text{ (MPa)} \end{cases} \quad (4)$$

, where σ_c and ϵ_c are the compressive stress and strain of concrete, respectively, f'_{cc} is the concrete effective compressive strength as influenced by confinement, ϵ'_{cc} is its equivalent strain, and E_c is the concrete elasticity modulus.

The AB, BC and CD parts of the stress-strain curve are according to the model presented by Tomii and Sakino (1979) as illustrated in Eq. (5)

$$\sigma_c = \begin{cases} f'_{cc} & \epsilon'_{cc} < \epsilon_c \leq 0.005 \\ \beta_c f'_{cc} + 100(0.015 - \epsilon_c) & 0.005 < \epsilon_c \leq 0.015 \\ \beta_c f'_{cc} & \epsilon_c > 0.015 \end{cases} \quad (5)$$

, where f'_{cc} is the concrete effective compressive strength,

which depends on the size of steel tube, concrete quality, and the amount of loading, which is calculated using Eq. (6) (Liang 2009).

$$f'_{cc} = \gamma_c f'_c \quad (6)$$

$$\gamma_c = 1.85 D_c^{-0.135} \quad (0.85 \leq \gamma_c \leq 1.0)$$

, where D_c is the diameter of the concrete core. In rectangular cross sections, the larger number between the two expressions of $(D - 2t)$ and $(B - 2t)$ is taken, where D , B and t are the length, width and thickness of the steel tube rectangular cross section, respectively. β_c coefficient is calculated using Eq. (7) (Liang 2009).

$$\beta_c = \begin{cases} 1 & D/t < 24 \\ 1.5 - D/t & 24 \leq D/t \leq 48 \\ 0.5 & D/t > 48 \end{cases} \quad (7)$$

As shown in Fig. 3, in defining the concrete tension behavior, it is assumed that before concrete cracking occurs, as tensile stress increases, the strain is raised linearly and after the concrete cracking, the tensile stress is linearly decreased to zero. Concrete tensile strength is taken as $0.6 \sqrt{f'_c}$ and the ultimate tensile strain is assumed as 10 times of the equivalent strain while cracking (Liang 2009). In the present study, the equivalent strain of concrete cracking was taken as 0.0002.

8-node 3-D solid elements with reduced integration (C3DR) were used for modeling the concrete parts with three transitional degrees of freedom in each node. Due to geometric necessity, the elements' sizes used for the concrete part of the structure were different. However, the largest concrete element was $50 \times 50 \times 50$ mm, and the smallest was $20 \times 20 \times 20$ mm.

2.2 Modeling of steel materials

J2 plasticity model with isotropic hardening was used for modeling the non-linear behavior of steel faceplates in ABAQUS. Necessary parameters for modeling included: 1. elasticity modulus, 2. Poisson's ratio, and 3. uniaxial stress-strain values. In the present study, elasticity modulus of steel material was taken as 2.1×10^5 MPa, Poisson's ratio was 0.29, and stress and strain values of steel faceplates were assumed to be according to the stress-strain curves of the steel plate and the steel box resulting from the test results. For modeling tie bolts and studs and drawing the stress-strain curves of the bars after the yielding point, it was assumed that the stress from the yielding point with a slope of 1 percent of elasticity modulus reached to the ultimate stress defined in the software. 4-node shell elements with reduced integration (S4R) for modeling steel faceplates materials was used, where each node had 3 transitional degrees of freedom and 3 rotational degrees of freedom. Size of the steel faceplates elements was selected in a way that each of steel elements nodes could be matched precisely with the nodes of the opposite concrete elements, thereby reducing the computational processing time. Size of the steel plate elements was different. The largest element was 50×50 mm and the smallest one was 20×20 mm. For

modeling the tie bars, beam elements that had flexural, axial, shear, and torsion strength with three transitional degrees of freedom and three rotational degrees of freedom (B31) were used.

2.3 Modeling of contact and constraint

In the present study, the composite shear wall consisted of infill concrete and steel faceplates. To increase the accuracy of the results, the hard contact between the infill concrete and the steel faceplate in the normal direction was considered. In this type of contact, surfaces cannot penetrate each other, but they can be separated from each other. In the transverse direction, for modeling the friction between the two surfaces, a surface-to-surface penalty-based formulation with the friction coefficient of 0.3 was used. Studs and tie bars were coupled by the infill concrete elements with the embedded constraint, and the slip between bars and concrete was ignored. A node-to-surface constraint was used to constrain the tie bars and studs to the steel faceplates.

2.4 Boundary conditions

Boundary conditions were applied to model the fixed base cantilever wall and lateral monotonic loading was imposed at the top of the wall as displacement-control; also, and axial compressive loading was modeled as the force-control using rigid beam and applied in the upper region of the composite shear wall. For the simultaneous displacement of steel and the infill concrete part, in the upper region of the wall, the surroundings of the steel part was tied to the infill concrete.

3. Definition of ductility capacity

In this study, the behavior of the composite shear wall was modeled and evaluated with regard to the initial stiffness, ductility, lateral strength and energy dissipation capacity. Ductility is defined as the structure capability to resist plastic deformation without any significant strength loss; and it is equal to the ratio of yielding displacement to ultimate deformation. The equivalent displacement of 0.85 of the ultimate strength was assumed to be equal to ultimate wall displacement, and the yielding displacement was assumed to be as that shown in Fig. 4 (Zhang *et al.* 2016). The area under force-displacement curve represented the amount of absorbed energy by shear wall as influenced by deformation; so, the higher the capacity of the shear wall in absorbing the energy, the better the performance of the whole structure in intensive earthquakes.

4. Validation of the proposed FE model

In order to verify the presented numerical model, experimental results were used. In the present study, the selected composite shear wall for numerical modeling was SW5, which is one of the 5 specimens of composite shear walls studied by Ji *et al.* (2013) and subjected to the cyclic

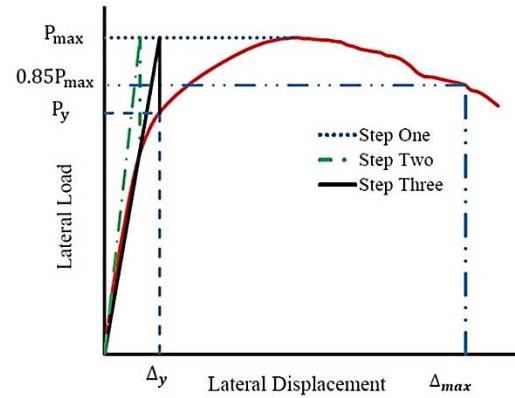
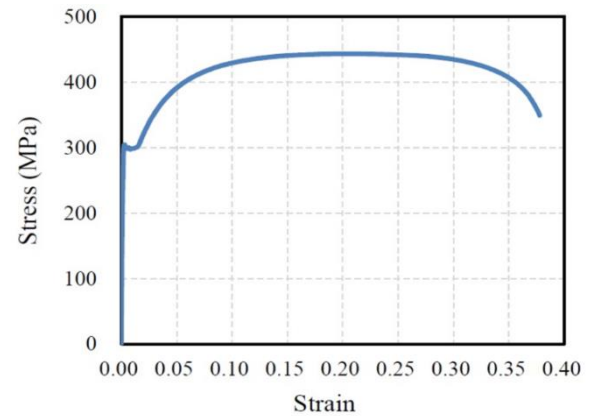


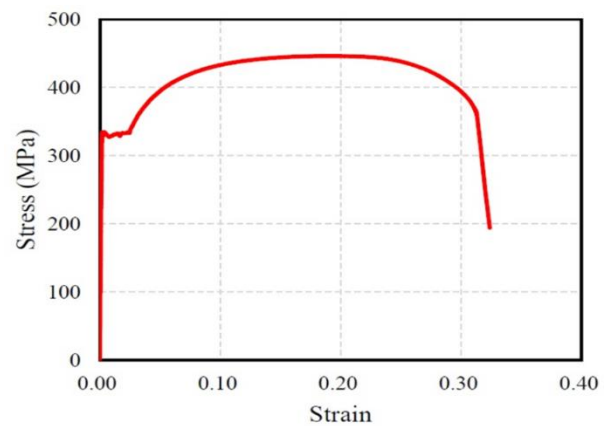
Fig. 4 Determination of yielding strength

Table 1 Properties of steel material (Data from Ji *et al.* 2013)

Steel material	Thickness/diameter (mm)	Yield strength (MPa)	Ultimate strength (MPa)
Steel plate	3	322.1	433.5
Steel tube	4	298.6	443.6
Tie bar	8	788.3	914.0



(a) Steel tube



(b) Steel plate

Fig. 5 Stress-strain curves of steel materials (Data from Ji *et al.* 2013)

lateral load and the compressive axial load. In the present study, the SW5 sample was named CSW. The height, length, and thickness of this specimen were 2600 mm, 1100

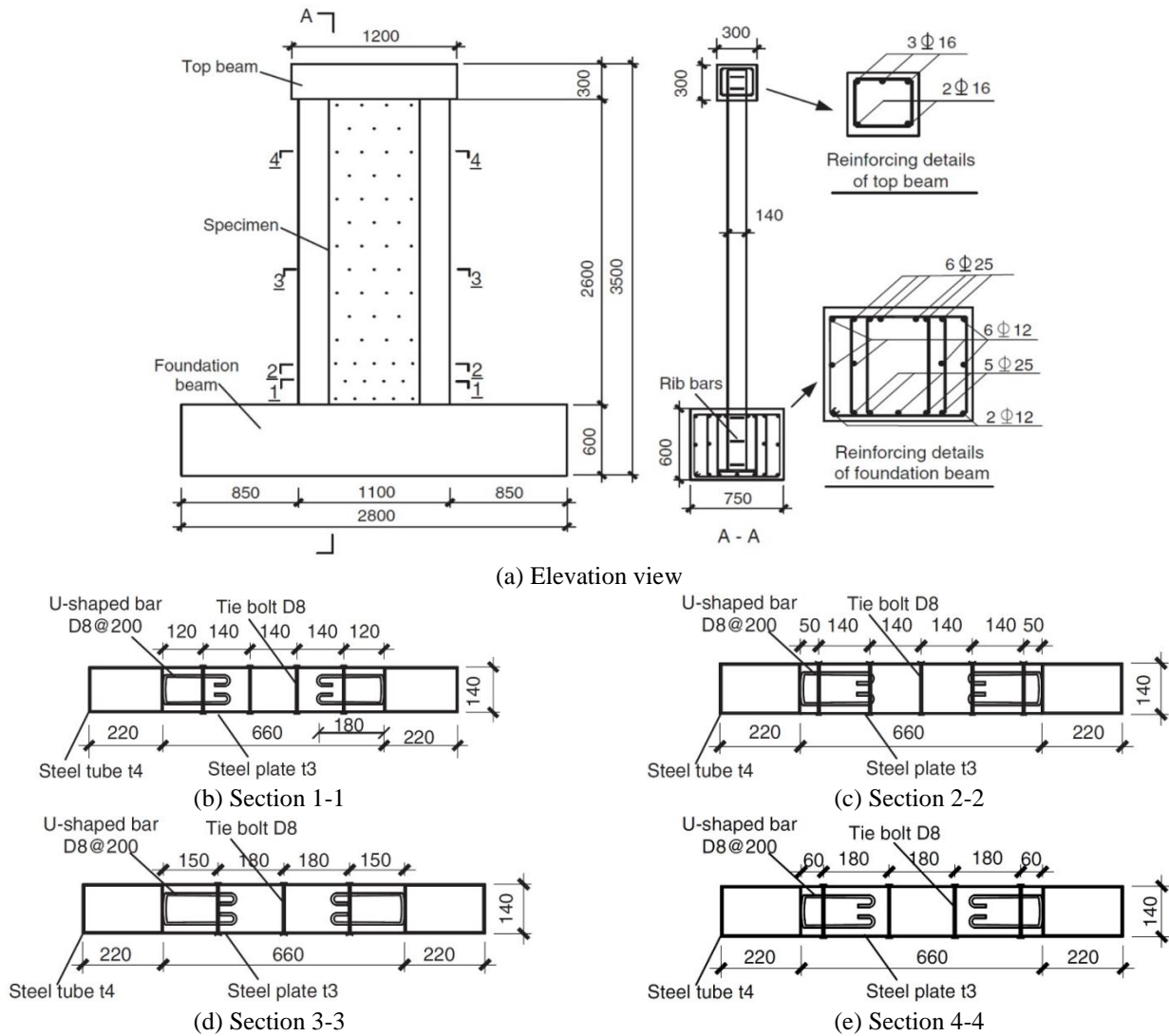


Fig. 6 Details of the selected composite shear wall tested by Ji *et al.* (2013)

mm and 140 mm, respectively. The wall consisted of two steel boxes, as boundary elements, and it was filled with concrete and two steel plates facing each other in the steel boxes joined by using tie bars; the spaces between them was filled with concrete. Tie bars spacing in the bottom region of the wall was half the height of the wall section equal to 140 mm and in the upper region, it was 180 mm. In order to transfer the shear force between steel boxes and infill concrete, U-shaped bars with 200 mm spacing were used. The applied compressive axial load to the specimen was 1431 kN and concrete compressive strength was 31 MPa. Details of steel materials, steel plate stress-strain curves, and steel boxes were assumed as those shown in Table 1 and Fig. 5, respectively. Fig. 6 demonstrates the details of the composite shear wall.

The tested specimen was numerically modeled using ABAQUS finite element software. Fig. 7 shows the results of numerical analysis and the resulting envelope curve of the hysteresis loops of the composite shear wall. Figs. 8 and 9, respectively, show the lateral deformation of the steel section and the plastic strain of the concrete part along the y-axis. In Fig. 9, the dark area shows compressive damage

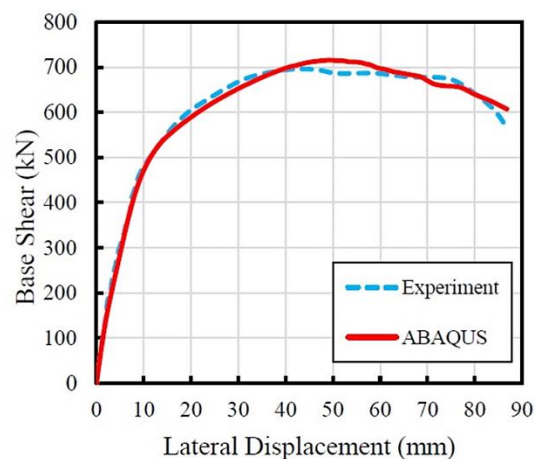


Fig. 7 Numerical modeling results and the envelope curve resulting from the cyclic response of the tested shear wall by Ji *et al.* (2013)

and the light area represents tensile damage in the infill concrete in the y-axis. Plastic strain inconsistency in concrete was the result of the slip between concrete and

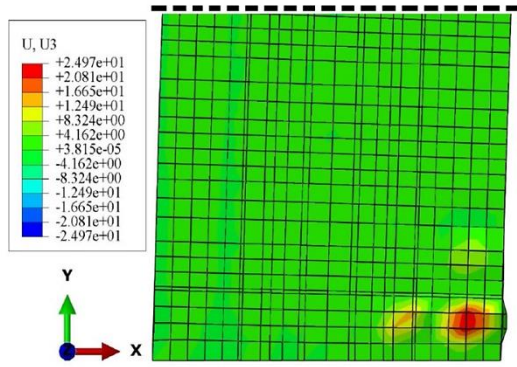


Fig. 8 Lateral deformation of steel in the compression Zone

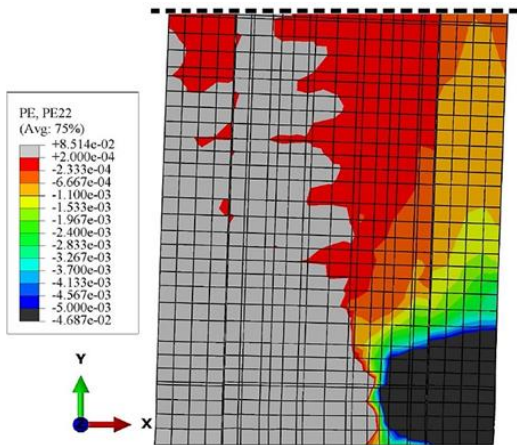


Fig. 9 Plastic strain of infill concrete in y-axis

steel plates. For example, Fig. 10 shows that the vertical displacement of nodes in the center of wall thickness on the exterior surface of compressive column was not the same for the concrete and the steel part. The comparison of the experimental and numerical results showed the adequate accuracy of the presented numerical model. By using this method, the ultimate lateral strength of the composite shear wall was increased to 715.47 kN, in comparison with the measured 702 kN in the experimental test, which showed 1.9% error.

5. Parametric studies

Having used the numerical model for the reference specimen (tested), we studied the effect of different parameters on the seismic behavior of the composite shear wall.

5.1 The effect of the tie bar diameter

In order to study the effect of the tie bar diameter on the seismic performance of the tested specimen (CSW), the two specimens CSW-D=10 mm and CSW-D=25 mm, whose tie bar diameter was 10 mm and 25 mm, respectively, were modeled. As shown in Fig. 11, the increase in the tie bar diameter from 8 mm to 25 mm did not influence wall behavior, but it slightly increased its

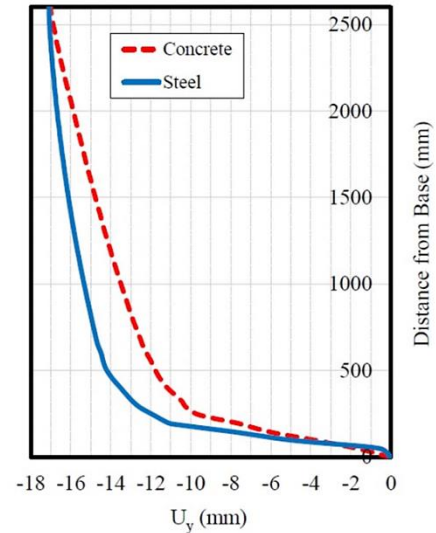


Fig. 10 The difference between the vertical displacement of concrete and steel faceplate in the center of wall thickness on the exterior surface of the compressive column

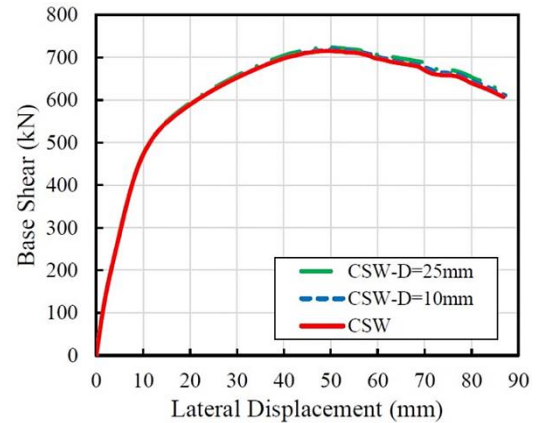


Fig. 11 Comparison of load-displacement curves for specimens with different tie bar diameter

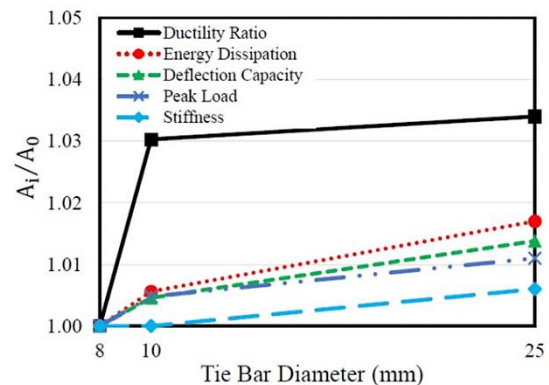


Fig. 12 The effect of the tie bar diameter on the seismic parameters of specimens

strength. After reaching the ultimate strength point of force-displacement curve, where the strain of steel faceplates was expanded, an increase in the axial stiffness of tie bars resulted in a decrease in the lateral displacement of steel faceplates and a slight increase in the ultimate strength of

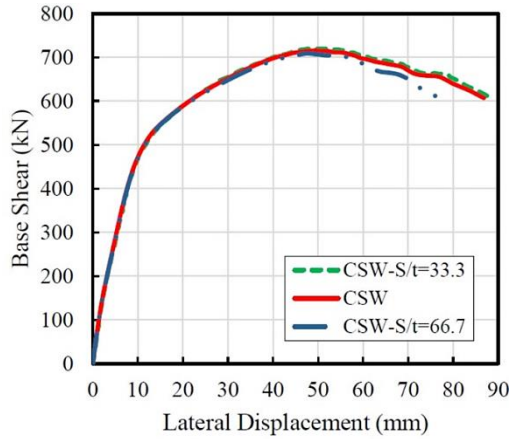


Fig. 13 Comparison of load-displacement curves for specimens with different tie bar spacing

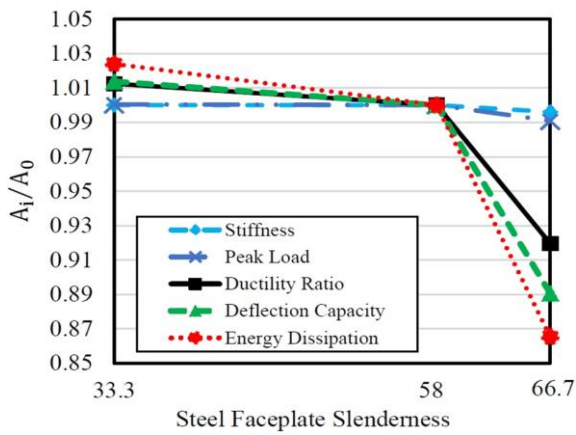


Fig. 14 The effect of the tie bar spacing on the seismic parameters of specimens

the composite shear wall. Fig. 12 shows that vertical axis (A_i/A_0) represents the ratio of the seismic parameters of the simulated specimen to the tested specimen; the main effect of tie bars diameter was on the composite shear wall ductility ratio.

5.2 The effect of tie bar spacing

Steel faceplate slenderness in composite shear walls is equal to the ratio of the spacing between tie bars to the thickness of steel faceplates. In the tested wall, the tie bars spacing in the bottom region of the wall was half the width of wall, equal to 140 mm; and in the upper region, it was 180 mm. Therefore, the slenderness of steel faceplates in the bottom region of the reference wall was equal to 46.7 and in the upper region, it was 60; on average, throughout CSW, it was equal to 58. In order to study the effect of spacing between tie bars on the performance of the composite shear wall, the two specimens of CSW-S/t=66.7 and CSW-S/t=33.3 were modeled; S/t was steel faceplate slenderness throughout wall height and the diameter of tie bars, according to the reference specimen, was 8 mm. According to Fig. 13, the results of the numerical analysis showed that steel faceplate slenderness was decreased from 60 to 33 in the upper region of the wall and from 47 to 33 in

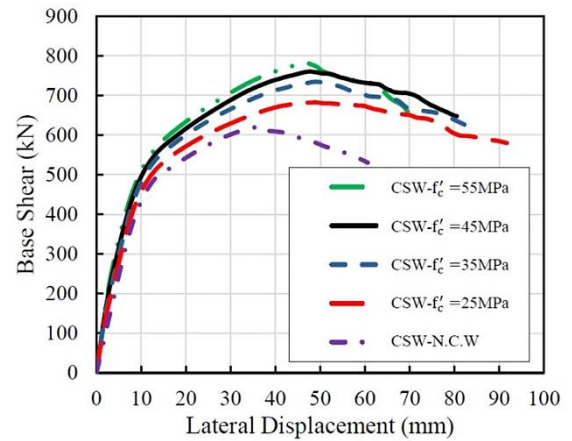


Fig. 15 Comparison of load-displacement curves for specimens with different concrete compressive strength

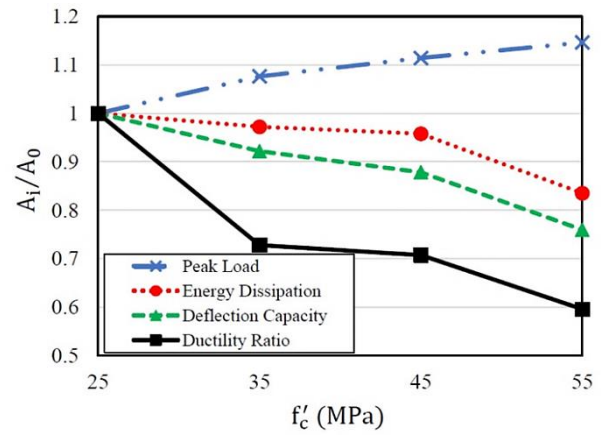


Fig. 16 The effect of the concrete compressive strength on the seismic parameters of specimens

the bottom region of the wall; this did not influence wall performance; that was because the spacing of tie bars in the reference specimen for preventing the elastic buckling of steel faceplates was adequate. However, in the specimen of CSW-S/t=66.7, the spacing of tie bars in the upper region of the wall was equal to 200 mm, which was approximately equivalent to the same amount in the reference wall, which was 180 mm. It can be assumed that by ignoring the difference, the wall performance was influenced by decreasing the tie bar spacing in the bottom region of the wall. By increasing it from 140 mm to 200 mm, wall strength and deformation capacity were decreased due to an increase in the length of steel faceplates buckling after the ultimate strength. According to Fig. 14, whose vertical axis (A_i/A_0) represents the ratio of the seismic parameter of the simulated specimen to the tested specimen, it was clear that decreasing the slenderness of steel faceplates had the most effect on the amount of the absorbed energy and the minimum effect on the lateral stiffness of the composite shear wall.

5.3 The effect of concrete compressive strength

In order to study the effect of concrete compressive strength on the performance of the composite shear wall,

the compressive strength of 25, 35, 45 and 55 MPa was evaluated. The specimens of CSW- $f'_c=25$ MPa, CSW- $f'_c=35$ MPa, CSW- $f'_c=45$ MPa, and CSW- $f'_c=55$ MPa were modeled according to the reference specimen; the compressive strength of the infill concrete and columns were assumed to be equal. Figs. 15 and 16 show the analysis results. In the specimen of CSW-N.C.W, to evaluate the effect of concrete between steel faceplates on the performance of the composite shear wall, by preserving the existing concrete in the lateral columns with the compressive strength of 31 MPa, no concrete between steel faceplates was modeled. According to Fig. 16, which compares the changes in the seismic indices of the specimen to CSW- $f'_c=25$ MPa, it could be seen that increasing the compressive strength of infill concrete resulted in decreasing the ductility, deformation capacity and energy dissipation, while stiffness and the lateral strength of the composite shear wall were decreased. By omitting the concrete layer, the ultimate strength was only decreased to 13.2%, as compared to the reference specimen (CSW); however, the deformation capacity of 30.2%, the ductility coefficient of 33.2%, and the capacity of energy absorption in the composite shear wall were decreased to 41.9%, as compared to the reference specimen. Therefore, it could be concluded that the main role of the concrete layer was preventing steel faceplates buckling.

5.4 The effect of concrete layer thickness

The concrete layer thickness in the reference specimen was 140 mm. In order to study the effect of the concrete layer thickness on the performance of the composite shear wall, the specimen of CSW- $t_c=50$ mm, whose infill concrete layer thickness was 50 mm, was modeled; then the results were compared with those of the reference specimen with no infill concrete. Fig. 17 shows the force-displacement curve in the composite wall with infill concrete and the thickness of 50mm, and the wall with no infill concrete. Up until the yielding point, the presence of concrete did not have much influence on the wall performance; at this point, buckling strength of steel faceplates did not occur, so it could be concluded that the main role of the infill concrete was preventing the buckling of steel faceplates. However, after reaching the ultimate strength point and the expansion of buckling of steel faceplates, the presence of the concrete layer had a significant effect on improving the deformation capacity and the composite shear wall ductility ratio. Fig. 18 shows the changes in the seismic indices of CSW- $t_c=50$ mm and the specimen with no infill concrete (CSW-N.C.W), as compared to the reference specimen (CSW).

5.5 The effect of steel faceplate thickness

As previously mentioned, the main role of infill concrete was to prevent buckling of steel faceplate, and increasing the thickness and compressive strength of concrete did not have any significant influence on increasing the strength and lateral stiffness; however, it mainly improved deformation capacity, ductility, and the composite shear wall energy absorption. In the tested specimen, the thickness of steel faceplate (t_p) was 3 mm, and the thickness

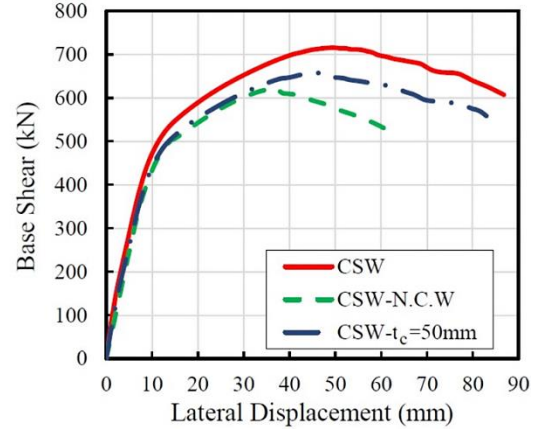


Fig. 17 Comparison of load-displacement curves for specimens with different infill concrete thickness

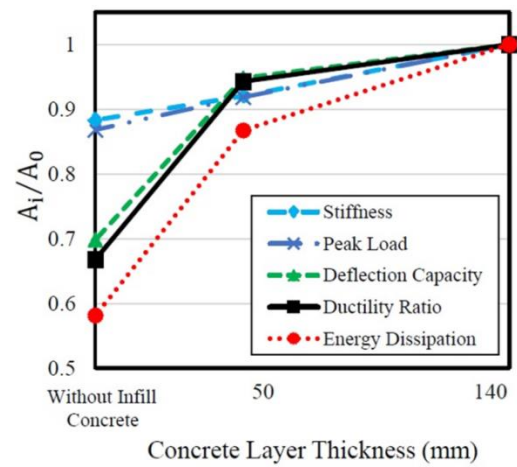


Fig. 18 The effect of the concrete layer thickness on the seismic parameters of specimens

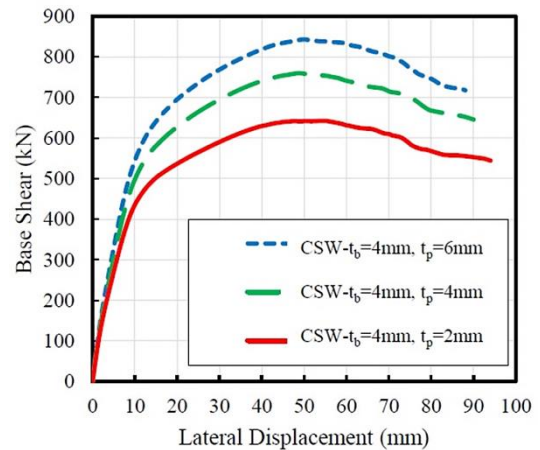


Fig. 19 Comparison of load-displacement curves for specimens with different steel plate thickness

of steel tubes (t_b) was 4 mm. In this part, the thickness of steel tubes, according to the reference specimen, was not changed; in order to study the effect of steel faceplates on the performance of the composite shear wall, the thicknesses of 2, 4 and 6 mm were evaluated. The specimens of CSW- $t_b=4$ mm, $t_p=2$ mm, CSW- $t_b=4$ mm, $t_p=4$

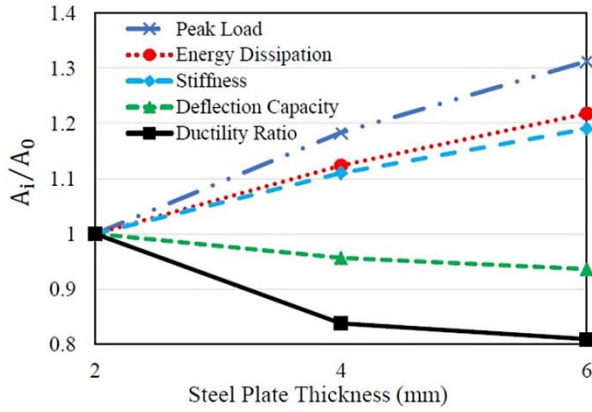


Fig. 20 The effect of the steel plate thickness on the seismic parameters of specimens

mm and CSW- $t_b=4$ mm, $t_p=6$ mm were modeled and all the specifications of the specimen except the steel plate thickness remained the same as the tested wall. Fig. 19 represents the simulated specimen force-displacement curve, showing that an increase in the steel plate thickness resulted in a significant increase in the lateral strength. According to Fig. 20, that shows changes in the seismic indices of the modeled specimens of CSW- $t_b=4$ mm, $t_p=2$ mm, an increase in steel plate thickness resulted in improving the stiffness and energy dissipation capacity, and decreasing the ductility and deformation capacity of the composite shear wall. Also, by comparing the results of compressive strength and thickness of infill concrete with those of steel faceplates thickness, it could be concluded that the role of steel faceplates in stiffness and strength was much more than that of the infill concrete.

5.6 The effect of local strengthening

As buckling of steel faceplates and concrete crushing can occur at the base of the shear wall, by strengthening the bottom regions of the composite shear wall by increasing the thickness of steel materials, the effect of local strengthening on the wall performance was evaluated. For modeling the specimen of this part, the reference wall was used. According to Fig. 21, in the steel section of the wall with the height of 400 mm and 800 mm from the base, that was 15.4% and 30% of the wall height, respectively, steel faceplates of higher thicknesses rather than the reference specimen were used, and the upper region was the same as the reference specimen. For instance, steel faceplate thickness in the bottom region of the composite wall (t_s) for the specimen of CSW- $H_s=400$ mm, $t_s=8$ mm was 8 mm. the specifications of other specimens were: CSW- $H_s=400$ mm, $t_s=10$ mm, CSW- $H_s=400$ mm, $t_s=12$ mm, CSW- $H_s=800$ mm, $t_s=8$ mm, CSW- $H_s=800$ mm, $t_s=10$ mm, CSW- $H_s=800$ mm, $t_s=12$ mm and CSW- $H_s=800$ mm, $t_s=14$ mm.

Fig. 22 shows the force-displacement curve of the strengthened specimens, as compared to the reference specimen (CSW). Figs. 23 and 24, respectively, show the changes in the seismic indices of the strengthened specimen with the height of 400 mm and 800 mm from the base

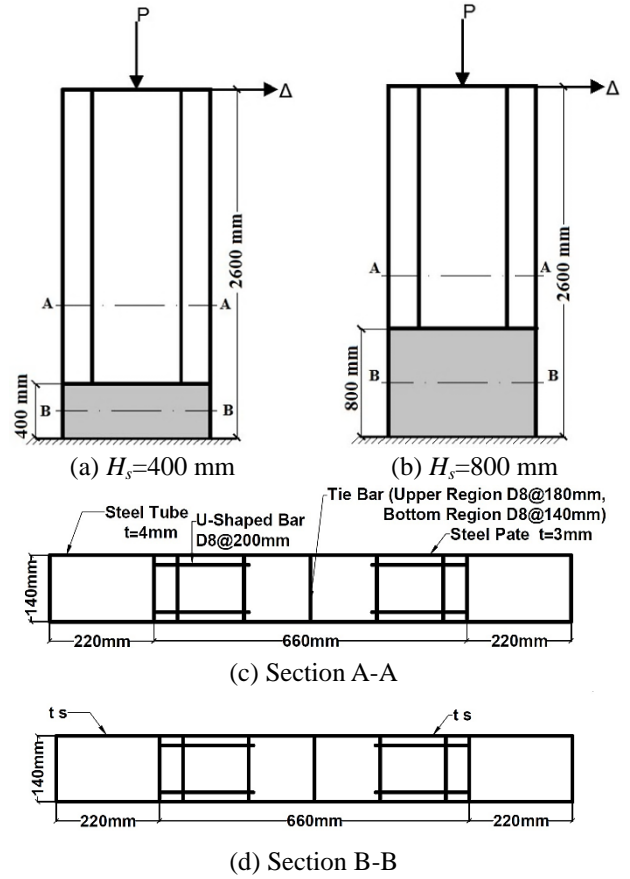


Fig. 21 Details of the strengthened specimens

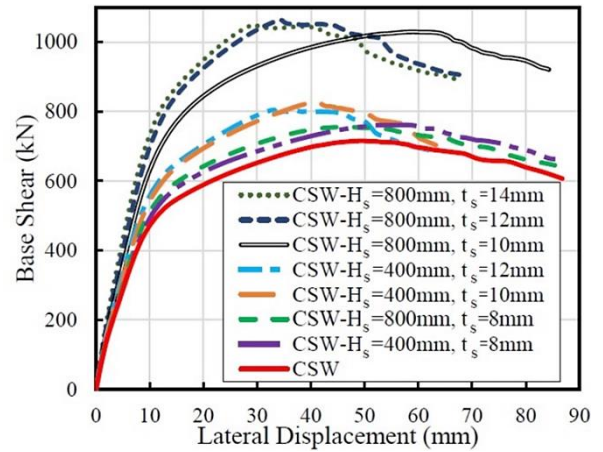


Fig. 22 The effect of strengthening the bottom region on the composite shear wall performance

support, as compared to the equivalent indices of the reference specimen (CSW). It could be concluded that by enhancing the thickness of steel faceplates in the strengthened part, the lateral strength was increased. However, the ductility and energy dissipation capacity of the composite wall were decreased. It could also be seen that as the thickness of the bottom region of the wall was increased to 10 mm for the height of 400 mm and the thickness of 12 mm for the height of 800 mm, the composite shear wall ductility was decreased and the wall was affected by a snap fracture which was the result of the

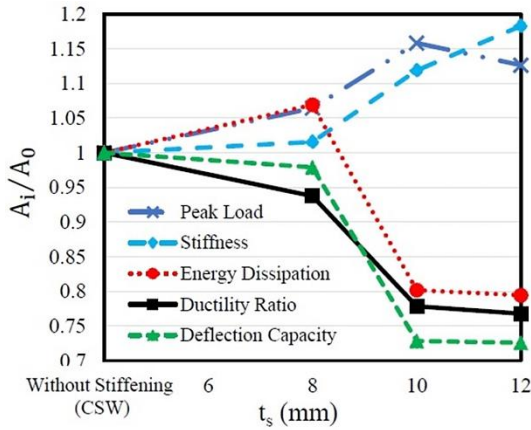


Fig. 23 The effect of strengthening the 400 mm height of bottom region on the seismic parameters of the composite shear wall

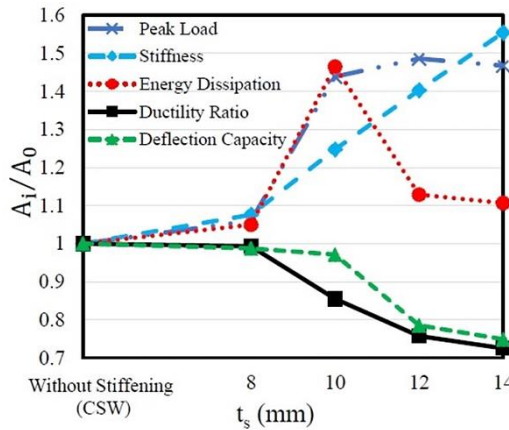
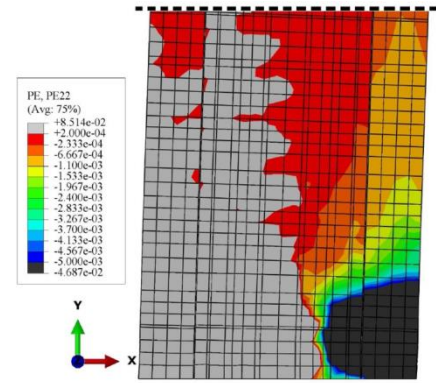


Fig. 24 The effect of strengthening the 800 mm height of bottom region on the seismic parameters of the composite shear wall

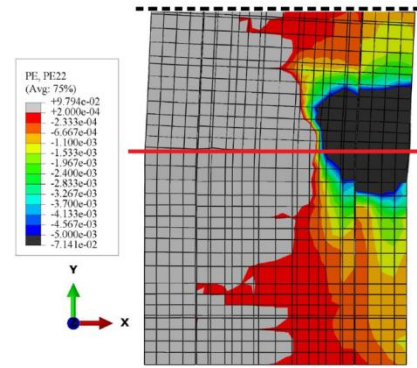
strengthened section of the wall as the support for the upper region of wall; by decreasing the ratio of height to length, a brittle fracture dominated the wall behavior. Also, the results of numerical analysis showed that by increasing the thickness of the bottom region of the wall, the lateral buckling of steel faceplates and concrete crushing ascended in the upper region of the strengthened section. As an example, the concrete section and the steel section of the specimen of CSW- $H_s=800$ mm, $t_s=14$ mm were compared to CSW at ultimate displacement, as shown in Figs. 25 and 26, respectively.

5. Conclusions

In this paper, non-linear finite element analysis was applied in order to evaluate the behavior of the composite shear wall consisting of steel faceplates, infill concrete and tie bars which tie steel faceplates together, and concrete filled steel tubular (CFST) as boundary columns. Then the effects of some mechanical and geometric parameters on the seismic behavior of the composite shear wall were studied.

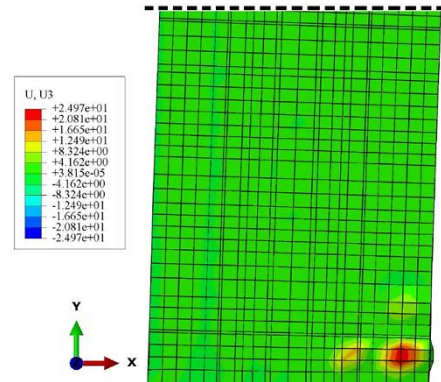


(a) CSW

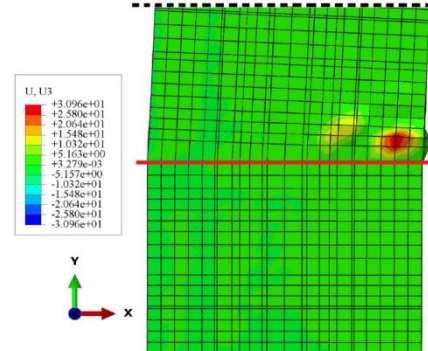


(b) CSW- $H_s=800$ mm, $t_s=14$ mm

Fig. 25 Comparison of compressive damage (dark colors) and tensile damage in the infill concrete (light colors)



(a) CSW



(b) CSW- $H_s=800$ mm, $t_s=14$ mm

Fig. 26 Comparison of the location of steel face lateral buckling

The key findings of the study can be summarized here:

- Diameter of the tie bars had an insignificant effect on the composite shear wall performance and a minimal tie bar diameter was necessary for preventing steel faceplates buckling.
- Increasing tie bar spacing resulted in decreasing the lateral strength, ductility, deformation capacity, and energy dissipation capacity of the composite shear wall; however, the decrease in energy absorption was the most prominent among others, and it was 13.5 percent. Additionally, altering the tie bar spacing did not have any effect on the wall lateral stiffness.
- Increasing the compressive strength of the infill concrete resulted in increasing the strength and the lateral stiffness of the wall; however, for the compressive strength of 55 MPa, the drop in the lateral strength after the ultimate strength point was more than that for the wall with the concrete compressive strength of 45 MPa. Also, increasing the concrete compressive strength resulted in decreasing the wall ductility.
- Removing the infill concrete of the wall resulted in a substantial decrease in wall strength and ductility. Also, the buckling pattern of steel faceplates was changed.
- Increasing the thickness of both infill concrete and steel plate resulted in increasing the stiffness and the lateral strength of the composite shear wall. However, the effect of steel faceplates thickness was much more than that of the infill concrete thickness. Also, studying the effect of concrete compressive strength on the wall performance showed that the composite shear wall was basically a steel shear wall in which the main role of infill concrete was preventing steel faceplate buckling.
- Steel faceplate buckling and concrete crushing at the wall base showed that the composite shear wall performance was affected by this area and strengthening the bottom region of the composite shear wall, as long as the strengthening section did not have the supporting role, could improve wall behavior in terms of strength, ductility, deformation capacity, stiffness, and energy absorption capacity.
- Provided that the thickness of the bottom region of the wall acts as the supporter of the upper region, the tendency of the wall behavior to change from a ductile performance to a brittle one increases. On the other hand, ductility, deformation capacity and wall energy dissipation capacity may decrease significantly.

- Huang, Z. and Liew, J.Y. (2016), "Numerical studies of steel-concrete-steel sandwich walls with J-hook connectors subjected to axial loads", *Steel. Compos. Struct.*, **21**(3), 461-477.
- Ji, X., Jiang, F. and Qian, J. (2013), "Seismic behavior of steel tube-double steel plate-concrete composite walls: experimental tests", *J. Constr. Steel Res.*, **86**, 17-30.
- Liang, Q.Q. (2009), "Strength and ductility of high strength concrete-filled steel tubular beam-columns", *J. Constr. Steel Res.*, **65**(3), 687-698.
- Mander, J.B., Priestley, M.J. and Park, R. (1988), "Theoretical stress-strain model for confined concrete", *J. Struct. Eng.*, **114**(8), 1804-1826.
- Rafiei, S. (2011), "Behavior of double skin profiled composite shear wall system under in-plane monotonic, cyclic and impact loadings", Ph.D. Dissertation, Department of Civil Engineering, Ryerson University, Toronto, Ontario, Canada.
- Rafiei, S., Hossain, K.M.A., Lachemi, M., Behdinan, K. and Anwar, M.S. (2013), "Finite element modeling of double skin profiled composite shear wall system under in-plane loadings", *Eng. Struct.*, **56**, 46-57.
- Tomii, M. and Sakino, K. (1979), "Elasto-plastic behavior of concrete filled square steel tubular beam-columns", *Tran. Arch. Inst. JPN*, **280**, 111-122.
- Zhang, X., Qin, Y. and Chen, Z. (2016), "Experimental seismic behavior of innovative composite shear walls", *J. Constr. Steel Res.*, **116**, 218-232.

SF

References

- Behfarnia, K. and Shirmeshan, A. (2017), "A numerical study on behavior of CFRP strengthened shear wall with opening", *Comput. Concrete*, **19**(2), 179-189.
- Chen, L., Mahmoud, H., Tong, S.M. and Zhou, Y. (2015), "Seismic behavior of double steel plate-HSC composite walls", *Eng. Struct.*, **102**, 1-12.
- Epacakchi, S., Whittaker, A.S., Varma, A.H. and Kurt, E.G. (2015), "Finite element modeling of steel-plate concrete composite wall piers", *Eng. Struct.*, **100**, 369-384.
- Hu, H.S., Nie, J.G. and Eatherton, M.R. (2014), "Deformation capacity of concrete-filled steel plate composite shear walls", *J. Constr. Steel Res.*, **103**, 148-158.